

Research Article

Synthesis and Characterization of a New Collagen-Alginate Aerogel for Tissue Engineering

Abraham Muñoz-Ruíz,¹ Diana M. Escobar-García,² Mildred Quintana,³
Amaury Pozos-Guillén ^{1,2} and Héctor Flores ^{1,2}

¹Doctorado Institucional en Ingeniería y Ciencia de Materiales, Universidad Autónoma de San Luis Potosí, S.L.P., Mexico

²Laboratorio de Ciencias Básicas, Facultad de Estomatología, Universidad Autónoma de San Luis Potosí, San Luis Potosí, S.L.P., Mexico

³Instituto de Física, Universidad Autónoma de San Luis Potosí, San Luis Potosí, S.L.P., Mexico

Correspondence should be addressed to Héctor Flores; heflores@uaslp.mx

Received 9 August 2019; Revised 19 September 2019; Accepted 30 September 2019; Published 21 November 2019

Academic Editor: Hassan Karimi-Maleh

Copyright © 2019 Abraham Muñoz-Ruíz et al. This is an open access article distributed under the Creative Commons Attribution License, which permits unrestricted use, distribution, and reproduction in any medium, provided the original work is properly cited.

Scaffolds have been used as extracellular matrix analogs to promote cell migration, cell attachment, and cell proliferation. The use of aerogels and carbon-based nanomaterials has recently been proposed for tissue engineering due to their properties. The aim of this study is to develop a highly porous collagen-alginate(-graphene oxide) aerogel-based scaffold. The GO synthesis was performed by Hummers method; a collagen-alginate and collagen-alginate-GO hydrogel were synthesized; then, they were treated by a supercritical drying process. The aerogels obtained were evaluated by SEM and FTIR. Osteoblasts were seeded over the scaffolds and evaluated by SEM. According to the characterization, the aerogels showed a highly porous interconnected network covered by a nonporous external wall. According to the FTIR, the chemical functional groups of collagen and GO were maintained after the supercritical process. The SEM images after cell culture showed that a collagen-alginate scaffold promotes cell attachment and proliferation. The alginate-collagen aerogel-based scaffold could be a platform for tissue engineering since it shows adequate properties. Further studies are needed to determine the cell interactions with GO.

1. Introduction

The loss and damage of organs and tissues due to injuries/diseases has been a concern for clinicians over the years and has motivated the development of regenerative therapy strategies [1]. Currently, there are some therapeutic strategies to heal or replace damaged tissues, such as prosthetic implants, mechanical devices, organ transplantations, surgical reconstruction, and autologous transplants [2]; even though these therapeutic options have aided countless patients and influenced towards better life quality, they have disadvantages like rare sources, susceptibility to infection, possibility of immune system rejection, and uncertain long-term dealing with patients [2]. Tissue engineering (TE) using biomaterials/scaffolds could offer a possibility to overcome

this situation, being a potential alternative to replace tissues/organs in a safe and noninvasive manner.

Biomaterials (natural, synthetic, or hybrid) [2] are used to design scaffolds with particular properties [2, 3]. Earlier, biomaterials were inert, designed to elicit no response from the immune system; nowadays, with the growth of molecular and cellular biology, a new model for biomaterials design has emerged [4]: create materials to be used as a source of bio-signaling to stimulate and activate cells [5] inducing a specific cellular response [6] to produce tissue regeneration and restore the original functionality [4]. Different tissues in the body have different mechanical, electrical, or physical characteristics, and a single material might not fully mimic the properties of native tissues; therefore, hybrid materials made of multiple components can fulfil different requirements [6].

Any biomaterial requires particular properties like biocompatibility, suitable microstructure, desired mechanical strength, and degradation rate [7]; also, porous scaffolds with highly functional properties are desirable [3, 8] to supply a network and an initial support to the cells to attach, proliferate, differentiate, and finally create a new extracellular matrix (ECM) [5, 9, 10]. Biological-based (biopolymers) scaffolds are a suitable platform for TE [2, 4, 7] mainly due to their similarities with the ECM, as well as their innate chemistry and biological characteristics [4, 7]. ECM has specific components such as collagen, elastin, trace cell engaging proteins, fibronectin, and growth factors [11], being the main component collagen [3, 12, 13], which is a natural biopolymer [14] with innate biocompatibility [4], making it an attractive material for biomedical applications [3, 4]; nevertheless, specific properties of collagen and its derivatives have adversely influenced some of its applications, like poor dimensional stability, poor in vivo mechanical strength, and relative low elasticity [15]; improvement of the physical characteristics of collagen to be used as biomaterial is required [14] and has motivated the study of collagen in combination with other compounds like carbon-based nanomaterials [16].

Graphene oxide (GO) is a subclass nanomaterial from the graphene family [6, 17]; it is an oxidized form of chemically modified graphene [18, 19]. It is made out of a single-atom-thick layer of carbons with carboxylic acid, oxygen (-O-), and hydroxyl (-OH) groups in its edges [18–22] and oxygen and hydroxyl groups on the basal plane [18, 20] allowing chemical interactions, hydrogen bonding, and other surface reactions [18]. GO has the capability to upregulate the degree of proliferation and differentiation of cultured cells, suggesting that GO is a biocompatible substrate [23]; besides mechanical properties of graphene and its derivatives, it could be used to reinforce TE scaffolds [18].

Recently, the use of aerogels as TE scaffolds has been proposed due to their mechanical properties, high specific surface area, and large pore volume. Aerogels are defined as networks of interconnected particles [24] with an intact solid structure without pore collapse, in which 90–99% is air by volume. The high porosity provides adequate microscopic and macroscopic structural features for TE [25].

Considering the limitations with current therapies, it is necessary to develop and evaluate new biomaterials/scaffolds that contribute to a rapid and effective tissue regeneration in order to obtain functional tissues. Different biopolymer-based aerogels have been reported to be used as TE scaffolds; nevertheless, there are limitations with its application, mainly related with mechanical properties [15]. Collagen is the main component of the ECM [3, 12, 13], which defines the architecture, signaling, and biomechanics of the cellular microenvironment [26], allowing access and fast diffusion of ions and molecules [27] and promoting cell migration [8].

Since the use of collagen and alginate as separated biomaterials showed adequate results, the combination of both with GO could improve their properties [28]. The aim of this study is to develop a new/novel highly porous collagen-alginate aerogel-based scaffold for TE.

2. Materials and Methods

2.1. Synthesis of GO. The GO synthesis was performed by an improved Hummers method [29, 30]. Briefly, a solution of H_2SO_4 (97%) + H_3PO_4 (85%) ((9:1) (360 mL of H_2SO_4 + 40 mL of H_3PO_4)) was prepared; the reaction was cooled using ice; then, a mixture of graphite powder and KMnO_4 powder ((1:6) (3 g of graphite + 18 g of KMnO_4)) was added to the solution and stirred at 500 RPM for 12 h; the solution was heated at 50°C and stored at room temperature for 2 h. Later, 3 mL of H_2O_2 (50%) was added, allowing the mixture to precipitate (48 h); the resultant supernatant was removed; the solution was centrifuged (1500 RPM, 1 h), and the supernatant was removed; shortly after, 200 mL of H_2O was added and stirred (1 h), the solution was centrifuged (3000 RPM, 1 h), and the supernatant was removed; the pH was set at 5 by water wash; then, 200 mL of HCl (33%) was added and stirred (10 min), the solution was centrifuged (3000 RPM, 2 h), and the supernatant was removed; the pH was set at 7 by water wash; 200 mL of ethanol was then added and stirred (10 min), later the solution was centrifuged (3000 RPM, 2 h), and the supernatant was removed; 200 mL of ether was added, and the solution was vacuum dried; the remaining material was pulverized to obtain a fine dust; finally, the GO was purified by repeating the water wash process. The GO produced was characterized by TEM, Raman, FTIR, and UV-Vis.

2.1.1. TEM of GO. The obtained images (Figure 1) correspond to self-folded monosheets of GO; the self-folded structure is formed due to the incorporation of functional groups into the structure of graphene when chemically synthesized.

2.1.2. Raman Spectra of GO. Raman spectroscopy provides a structural characterization of carbon materials [31]. The Raman spectra (Figure 2) were collected using an excitation wavelength of 514 nm. The spectra showed peaks at 1600 nm and 1350 nm, corresponding to the D peak and G peak of the GO, respectively, confirming the presence of GO [29, 31].

2.1.3. FTIR Spectra of GO. The FTIR spectra (Figure 3) present signal peaks associated to the functional groups [O-H] at 3420 cm^{-1} , [C=O] at $1720\text{--}1740\text{ cm}^{-1}$, [C=C] at $1590\text{--}1620\text{ cm}^{-1}$, and [C-O] at 1250 cm^{-1} . The obtained spectra corroborate the presence of GO [29].

2.1.4. UV-Vis Spectra of GO. The UV-Vis spectra (Figure 4) of GO showed a peak in the range of 227–231 nm as previously reported for GO [29].

2.2. Synthesis of Aerogel

2.2.1. Synthesis of Collagen-Alginate Hydrogel. The hydrogel synthesis was carried out according to the previously reported literature [12, 28, 32]. Briefly, 12 mg of collagen (rat tail tendon, type I, Sigma, St. Louis, MO) was dissolved in 2.5 mL of acetic acid (0.2%); the solution was exposed to UV light overnight; then, alginic acid (12.5 mg/mL), NaCl (8.76 mg/mL), and HEPES (4.76 mg/mL) were added; the solution was crosslinked with CaCl_2 ; finally, the hydrogel was washed with EDTA and H_2O . The hydrogel was stored

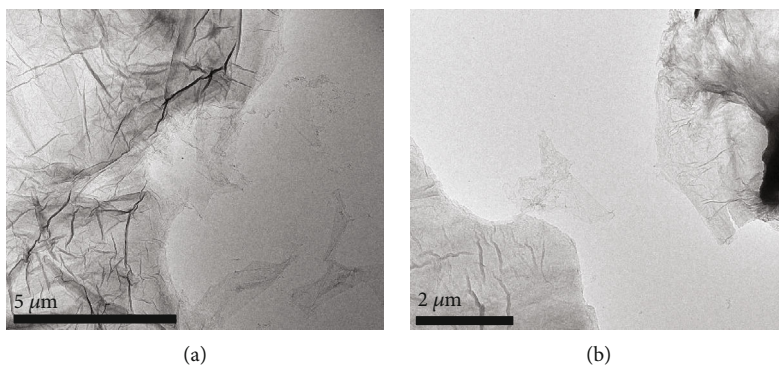


FIGURE 1: TEM of GO. (a) Self-folded monosheets produced due the incorporation of functional groups into the structure of graphene. (b) Observe the thickness of GO basal planes.

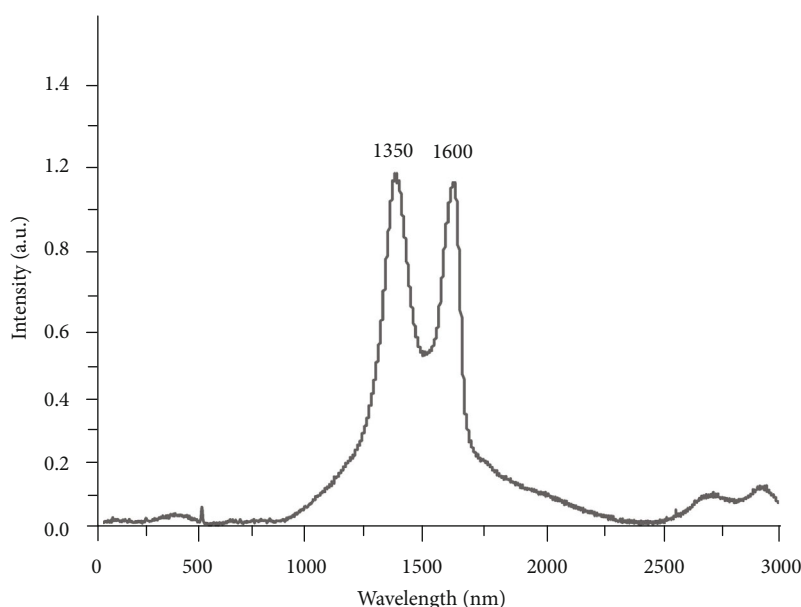


FIGURE 2: Raman spectra of GO (wavelength 514 nm). The spectra show peaks at 1600 nm and 1350 nm corresponding to the D peak and G peak of GO, respectively.

at -4°C until use. A collagen-alginate-GO hydrogel was synthesized following the previous methodology, incorporating 0.01 mg/mL of GO by sonication (5 min) previously to UV light exposition.

2.2.2. Water-Solvent Exchange of Hydrogel. Prior to the supercritical drying process, the water content of the hydrogels was replaced by ethanol according to previous literature reports [33]. The water-ethanol exchange was carried out using ethanol at 10%, 30%, 50%, 60%, 70%, 80%, 90%, and 100%; the hydrogels were embedded in each ethanol concentration for 1 h to perform the exchange. To confirm the water-ethanol exchange, a TGA test was performed.

2.2.3. Supercritical Drying. A supercritical dryer (manuclave) was handcrafted according to a design previously described in <http://aerogel.org> [34]. The hydrogels were loaded upon

a covered coil holder, which was placed inside the chamber of the manuclave; once the chamber was closed, it was filled with CO_2 and the system was set to reach a pressure of 750 PSI; the lateral needle valve was opened (15 min) to allow the CO_2 gas to pass to a liquid state, allowing it to be mixed with ethanol; then, the bottom ball valve was opened (10 min), letting the ethanol- CO_2 mixture escape the manuclave; then, manuclave was refilled with CO_2 and the lateral needle valve was opened (15 min). 24 h later, the bottom ball valve was opened (10 min) to release the CO_2 ; then, lateral needle valve was opened (15 min); this process was performed every 24 h for 3 days. Then, the system was set to supercritical state; briefly, the chamber was heated to 105°F , which raised the pressure to 1200 PSI; these conditions were maintained for 30 min; then, the temperature and pressure were increased to 120°F and 1400 PSI, respectively, and the system was allowed to stabilize (30 min); the lateral needle

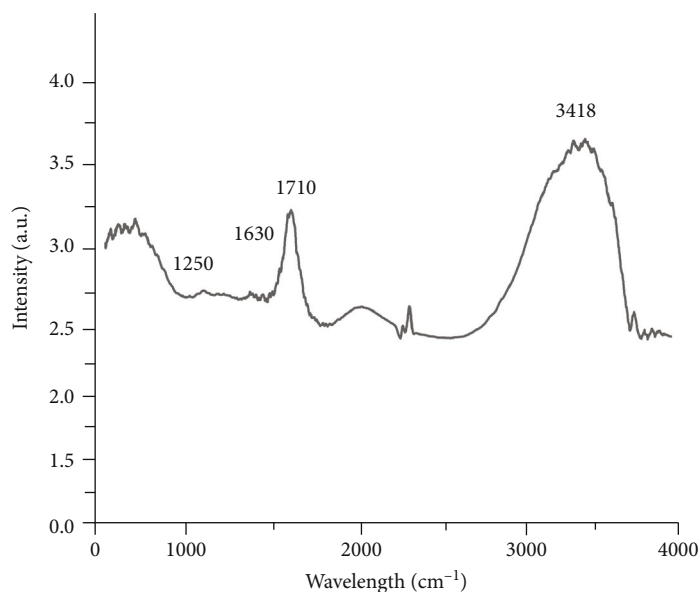


FIGURE 3: FTIR spectra of GO. The spectra show peaks at 3418 cm^{-1} , 1710 cm^{-1} , 1630 cm^{-1} , and 1250 cm^{-1} , corresponding to [O-H], [C=O], [C=C], and [C-O] functional groups of GO.

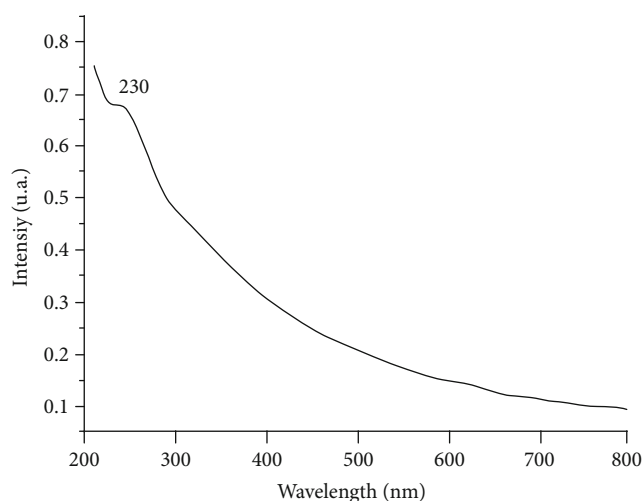


FIGURE 4: UV-Vis spectra of GO. The spectra show a peak at 230 nm, corresponding to GO.

valve was slightly opened, allowing the system to release 200 PSI in 20 min; then, the chamber was heated to 120°F , which raised the pressure to 1150 PSI approximately; the system was allowed to stabilize (30 min); finally, the system was depressurized by releasing the CO_2 over 60 min. Finally, the system was opened, and aerogels were collected.

2.3. Characterization of Aerogel. The aerogel characterization was done by SEM, FTIR, and a pycnometer.

2.4. Osteoblast Cell Culture. An osteoblast cell line was cultured over the collagen-alginate and collagen-alginate-GO aerogel-based scaffold in 96-well culture plates using DMEM containing penicillin (100 U/mL penicillin), streptomycin (100 mg/mL), and fetal bovine serum (10%). The cell culture

was incubated 48 h at 37°C and 5% CO_2 incubator. Then, samples were prepared for SEM analysis.

3. Results

3.1. Synthesis of Aerogel

3.1.1. Water-Solvent Exchange. Prior to the supercritical drying process, a water-solvent exchange was performed. A TGA test was performed to the hydrogels after and before the exchange process. According to data obtained (Figure 5), water-hydrogel displayed a major mass loss at 93.91°C and the alcohol-hydrogel at 72.55°C . The difference of mass loss between both samples is due to the boiling point of water at 100°C and the ethanol boiling point at 78.4°C . Considering that the major volume of the samples is water and alcohol, data obtained suggests that water-solvent exchange was carried out.

3.1.2. Supercritical Drying. The supercritical process produced three-dimensional collagen-alginate and collagen-alginate-GO aerogel-based scaffolds. The structure of the aerogels was stable; the dimensions of the aerogels compared to the hydrogel were similar, meaning that there was no collapse of the structure.

3.2. Characterization of Aerogel

3.2.1. SEM of Aerogels. The SEM images (Figure 6) of the aerogels showed a highly porous interconnected network covered by a nonporous external wall. The pores range from 2-10 micrometres.

3.2.2. FTIR Spectra of Collagen-Alginate-GO Aerogel. The FTIR spectra of the collagen-alginate-GO aerogel (Figure 7) showed peaks at 1209 cm^{-1} , 1551 cm^{-1} , and 1662 cm^{-1} that

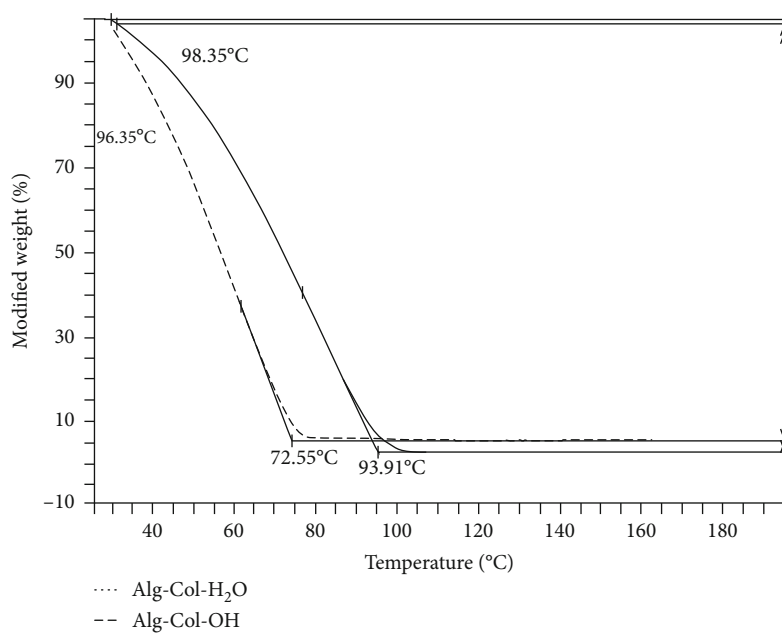


FIGURE 5: TGA spectra of hydrogels. The alginate-collagen sample shows a major mass loss at 93.91°C; the alginate-collagen water-ethanol exchange sample shows the major mass loss at 72.55°C.

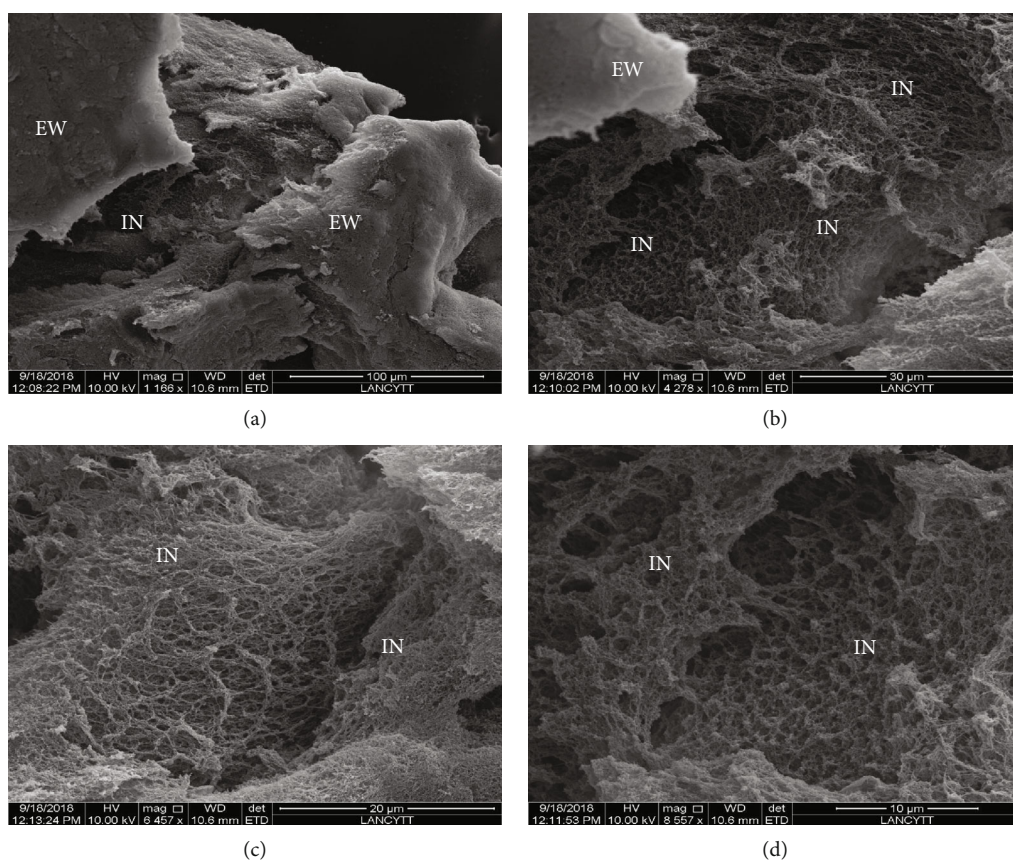


FIGURE 6: SEM of aerogels. (a) Highly porous interconnected network covered by a nonporous external wall (EW). (b–d) Notice a highly porous interconnected network (IN). The pores range from 2–10 micrometres.

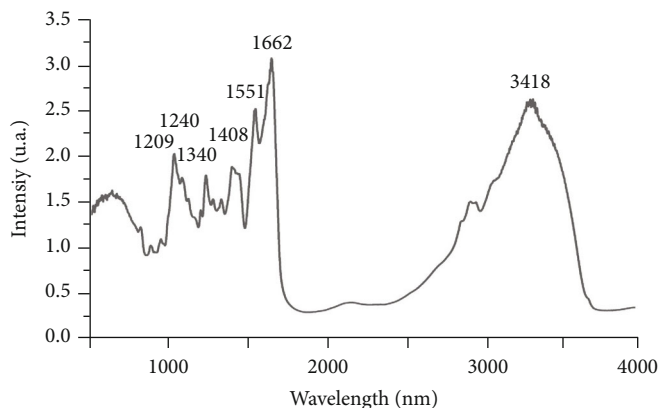


FIGURE 7: FTIR spectra of collagen-alginate-GO aerogel. The spectra show peaks at 1209 cm^{-1} , 1551 cm^{-1} , and 1662 cm^{-1} that correspond to amide band peaks of collagen and peaks at 1240 cm^{-1} , 1340 cm^{-1} , 1408 cm^{-1} , and 3418 cm^{-1} related to functional groups of GO.

correspond to the amide band I peak of collagen, suggesting that chemical properties of collagen were maintained even after the supercritical drying process and that biological properties of the biopolymer might have been maintained, and peaks at 1240 cm^{-1} , 1340 cm^{-1} , 1408 cm^{-1} , and 3408 cm^{-1} related to functional groups of GO [28].

3.2.3. Density Evaluation of Aerogels. A pycnometer was employed to determine the density of the aerogel. According to data obtained, density of the aerogels was 558.65 mg/mL .

3.3. Osteoblast Cell Culture. The SEM images (Figure 8) of the osteoblast culture at 48 h showed cell attachment, proliferation, and capability of interaction with the surface of the collagen-alginate aerogel-based scaffold; osteoblasts seeded had normal appearance with some filopodia extended to other cells and scaffolds. Also, nodules can be observed over some cells corresponding to ECM synthesis. The SEM images (Figure 8) of the osteoblast cell culture at 48 h over the collagen-alginate-GO aerogel-based scaffold showed low cell attachment and low cell proliferation; the osteoblasts seeded had an abnormal appearance with no filopodia extended to other cells or the scaffold surface, suggesting that GO incorporation could negatively affect cell response and interaction.

4. Discussion

This study describes a method to synthesize a new collagen-alginate aerogel-based scaffold for TE made by the supercritical CO_2 drying process. Different biopolymer-based aerogels have been reported to be used as TE scaffolds; nevertheless, there are some limitations with their use, mainly related with mechanical properties [15]. Nowadays, there has been considerable interest in carbon-based nanomaterials to fabricate a new class of materials with unique properties [20]. In this study, a method to improve the mechanical and biological properties of the scaffold by the incorporation of alginate and GO was used, since it has been previously reported as successful [6, 28, 35–37]. Even though it has been established that both materials could be employed to improve general properties of biomaterials, results in this study showed that

the incorporation of GO could negatively affect cell attachment, proliferation, and response. Further studies are needed to confirm this data.

Scaffold/biomaterials require properties like biocompatibility, suitable microstructure, mechanical strength, and degradation rate, as well as the feature to support cell residence and allow metabolic functions [7]. This study suggests an aerogel-based scaffold that could match these features, since aerogels have characteristics which make them ideal scaffolds for TE [8].

Aerogels are an interconnected network with a three-dimensional structure that results from chemical bonds formed between particles [24] in which the liquid component of the precursor gel has been replaced with a gas by an extraction process [24, 27] leading to the formation of a porous material with highly specific surface areas [24]. Even when porous scaffolds with highly functional properties are desirable for TE [3, 8], it is usually considered that most highly porous biomaterials are mechanically weak; mechanical stiffness of a native extracellular matrix is on the order of 100 MPa , and different aerogel formulations can easily match an adequate mechanical strength [8].

Supercritical drying is a technique that prevents formation of a liquid-vapor meniscus that recedes during the emptying of pores in wet gels. As in a supercritical fluid, liquid and vapor phase become indistinguishable and no capillary forces occur [25]. Compared to other drying methods, supercritical drying is a more effective method for preventing the shrinkage or collapse of mesopores [25]. The synthesized aerogel-based scaffold in this study showed a highly porous network and no collapse of the structure, in which the pores range from 2–10 micrometres; a similar structure is reported by Baldino et al. [36], who synthesized an alginate-gelatine aerogel by CO_2 supercritical method; they reported a nanofibrous structure, in which the nanofibers have a diameter lower than 100 nm . The similarity in the three-dimensional structure of the alginate-gelatine aerogel and the collagen-alginate-GO aerogel in this study could be due to the fact that gelatine is a protein compound obtained by partial hydrolysis of collagen and maintains most of its structure and amino groups [38]. Nevertheless, it has been reported that the

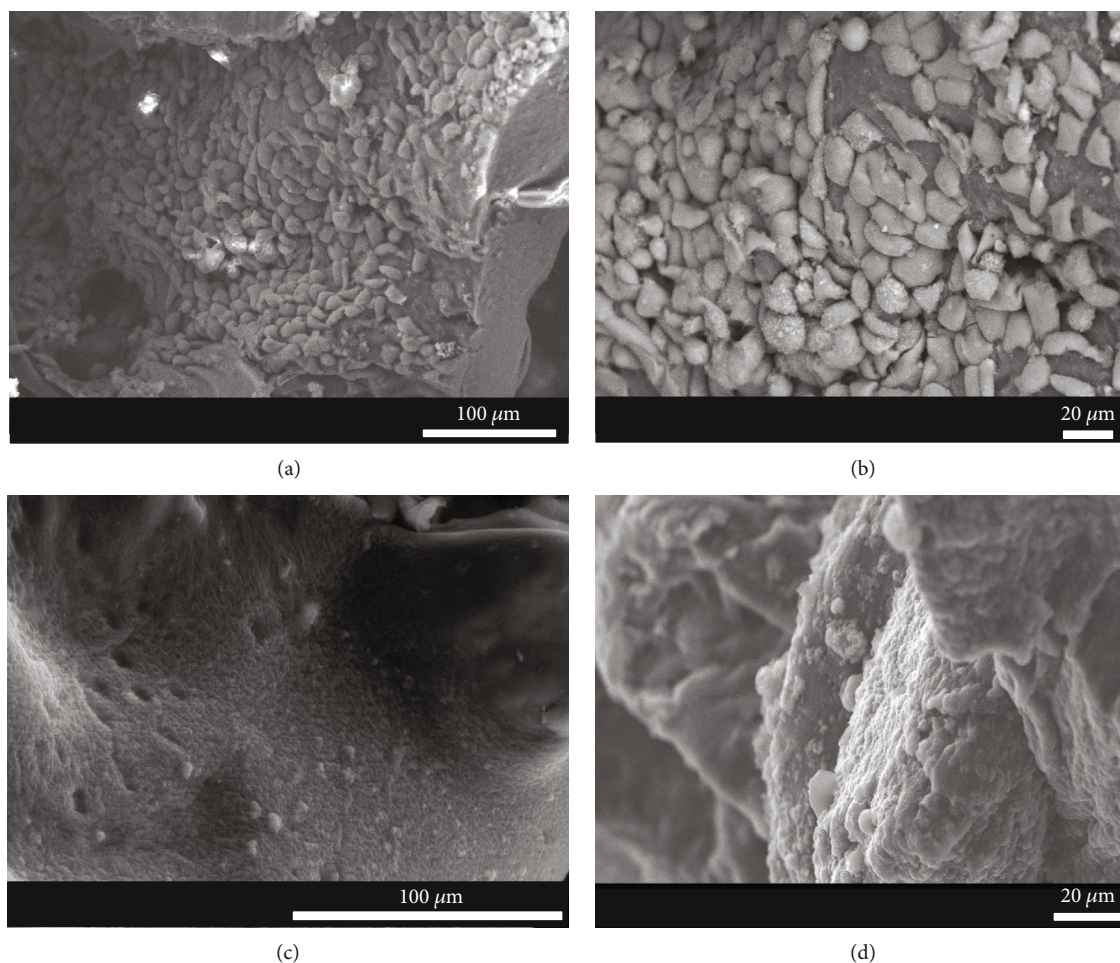


FIGURE 8: SEM of osteoblast cell culture at 48 h. (a, b) Cell attachment and cell proliferation can be observed over the collagen-alginate aerogel-based scaffold; osteoblasts seeded had a normal appearance with some filopodia extended to other cells. (c, d) Osteoblast cell culture at 48 h. Low cell attachment and low cell proliferation can be observed over the collagen-alginate-GO aerogel-based scaffold. Osteoblasts seeded had an abnormal appearance.

gelatine gelation mechanism, as well as the formed gel network structure, differs considerably from collagen, as described by Gomez-Guillen et al. [38]; despite this, the three-dimensional structure obtained by CO₂ supercritical method is similar in both combinations carried out in this study, probably because of the crosslinking performed previously in the hydrogel phase. Baldino et al. [36] also confirmed that the supercritical process does not modify the gel organization and avoids gel collapse during drying.

Martins et al. [35] reported an alginate-based aerogel for TE; to obtain an adequate porosity in the structure, Martins et al. proposed different pressuring and depressurizing rates. In this study, a collagen-alginate-GO aerogel with a highly porous structure is presented; the incorporation of collagen type I and the crosslinking performed by UV light allow a porous three-dimensional structure to be formed, even without the use of specific pressuring and depressurizing rates; also, the biological characteristics of collagen added to the aerogel provide adequate properties for its use in TE. On the other hand, the incorporation of alginate in our aerogel was employed to encapsulate the collagen into the alginate allowing an easy manipulation of the hydrogel prior to the

supercritical process. Collagen UV crosslinking relies on the reaction of aromatic groups (tyrosine and phenylalanine) [4]; this method does not rely on the amino acids found in integrin ligands, becoming a way to optimize scaffold strength while retaining cell compatibility [4]; preserving the ligands which communicate with cells is extremely important. It has been shown that crosslinkers that interfere with integrin ligands cause a significant decrease in cell attachment, proliferation, and migration [4]. Creating mixtures of collagen and other polymers has led to a wide range of biomaterials with differing biological properties [4]; in this study, collagen was mixed with sodium alginate in aqueous solution to form a hydrogel by divalent calcium binding [39].

The biocompatibility and the degradation rate of a scaffold depend on the based material of the aerogel [8]; since biocompatibility is typically determined by chemical composition and degradation products [8], natural biopolymers are attractive for biomedical applications [14]. Collagen is the main component of the ECM [3, 12, 13], which defines the architecture, signaling, and biomechanics of the cellular microenvironment [26]; ECM is on the order of 80% of porosity [8], allowing access and fast diffusion of ions and

molecules [27] and promoting cell migration [8], which is why a highly porous scaffold is desirable. According to SEM images of the collagen-alginate-GO aerogel-based scaffold, a highly porous interconnected network covered by a nonporous external wall was observed; this structure is favorable for TE since it allows normal cell metabolism due to its porosity, and the external wall could protect the collagen network during the initial phases of healing (inflammation) after the implantation of the scaffold.

Lu et al. [40] proposed the use of collagen-bacteria nanocellulose aerogels for wound dressing; according to their macroscopic view and SEM morphology, entangled nanofibers formed a free-standing three-dimensional structure, which is similar to the morphology of the aerogel described in this study; even when cellulose has proved to be effective in TE, the difficulty to obtain it and its controversial source could limit a clinical application. In this study, we propose the use of collagen type I as base biopolymer, which is the main component of the ECM in mammals [3, 12, 13], because it proved biocompatibility and biological characteristics [4], making it an attractive material for biomedical applications [3, 4].

GO was first prepared by Brodie in 1859 [41]; the original process was time-consuming and hazardous [41], but by using Hummers method, the entire process can be carried out safely and in less time [41]. Besides, GO in comparison to other carbon-based nanomaterials exhibits some merits like low cost of production and extremely large surface area [21], allowing many reactive sites for chemical functionalization and interactions [18, 22]. Also, it has been proved that GO can be used to improve mechanical strength of bioceramics, hydrogels, and bioactive glasses, without damaging their structures or altering biocompatibility [6].

In this study, GO was incorporated to the aerogel based on previous studies [6, 28, 37] to improve the biological and mechanical properties of the scaffold. Bazrafshan and Stylios [37] reported that the presence of GO could enhance the output of collagen-based nanocomposites during the synthesis in quality and quantity and proved that the incorporation of GO improved the physiochemical properties of collagen; Shin et al. [6] utilized graphene and GO sheets and demonstrated that they acted as a preconcentration platform for stem cell inducers; Sivaranjani and Pandimadevi [28] reported the use of a film of collagen-alginate-GO in wound healing; according to their SEM results, the surface of collagen-alginate was smooth and porous in nature, and even with the incorporation of GO, the scaffold had retained its porosity. Our results correlate to this data, since the incorporation of GO into the aerogel while it was in hydrogel phase did not affect or modify the porous network of the aerogel. Also, Sivaranjani and Pandimadevi [28] reported that increasing concentrations of alginate decreased the tensile strength of the films; also, when low concentrations of collagen were used, the film had the least tensile strength. The FTIR spectra of the films reported by Sivaranjani and Pandimadevi [28] reported the presence of the characteristic bands at 1632 cm^{-1} , 1547 cm^{-1} , and 1203 cm^{-1} of the amide peaks of collagen; the carboxyl peaks of alginate and GO at 1416 cm^{-1} and 1357 cm^{-1} , respectively; and the carbohydrate

groups present in collagen at 1241 cm^{-1} ; also, a peak loss at 1740 cm^{-1} is reported. Similar data were obtained in our study in which peaks at 1209 cm^{-1} , 1551 cm^{-1} , and 1662 cm^{-1} (amide band peaks of collagen) and peaks at 1240 cm^{-1} , 1340 cm^{-1} , 1408 cm^{-1} , and 3408 cm^{-1} (peaks of alginate and GO) were identified; also, a loss of the peak at 1710 cm^{-1} , related to the [C=O] functional group of GO, confirms the GO functionalization and chemical interaction with other aerogel components (collagen and alginate), corroborating the data reported by Sivaranjani and Pandimadevi. According to the literature, the combination of graphene and its derivatives with other compounds makes them candidates to fabricate multifunctional smart materials [6] thanks to the remarkable progress in the synthesis and functionalization of graphene materials [18]. However, further studies are needed to guarantee a safe use of these nanomaterials.

5. Conclusions

The use of hybrid biomaterials as an ECM analog represents an alternative to mimic the three-dimensional structure and properties of native tissues. Since alginate, collagen, and GO have been employed previously in the TE field with good results, it is logical to incorporate them to obtain a hybrid biomaterial. This study describes a method to synthesize a new collagen-alginate aerogel-based scaffold for TE made through the supercritical CO_2 drying process, producing three-dimensional collagen-alginate and collagen-alginate-GO aerogel-based scaffolds. The structure of the aerogels was stable. The microstructure of the aerogels consists of a highly porous interconnected network, which is favorable for cell attachment, proliferation, and metabolism/function. According to the FTIR, the aerogels do not show chemical modifications of the functional groups after the supercritical drying process. The SEM images of the osteoblast culture showed cell attachment, proliferation, and capability of interaction with the surface of the collagen-alginate aerogel-based scaffold. The cell culture over the collagen-alginate-GO aerogel-based scaffold showed low cell attachment and low cell proliferation. Further studies are needed to determine the cell interactions with GO.

Data Availability

The data that support the findings of this study are available from the corresponding author (HF) upon reasonable request.

Conflicts of Interest

The authors declare that there is no conflict of interest regarding the publication of this paper.

Acknowledgments

The authors are grateful for the financial support from a grant of PFCE-Universidad Autónoma de San Luis Potosí and PRODEP. Also, AMR wish to thank CONACYT for their doctoral scholarship (No. 289207) during this study.

References

- [1] A. S. Mao and D. J. Mooney, "Regenerative medicine: current therapies and future directions," *Proceedings of the National Academy of Sciences of the United States of America*, vol. 112, no. 47, pp. 14452–14459, 2015.
- [2] N. Mansouri and S. Bagheri, "The influence of topography on tissue engineering perspective," *Materials Science and Engineering: C*, vol. 61, pp. 906–921, 2016.
- [3] J. L. Drury and D. J. Mooney, "Hydrogels for tissue engineering: scaffold design variables and applications," *Biomaterials*, vol. 24, no. 24, pp. 4337–4351, 2003.
- [4] K. M. Pawelec, S. M. Best, and R. E. Cameron, "Collagen: a network for regenerative medicine," *Journal of Materials Chemistry B*, vol. 4, no. 40, pp. 6484–6496, 2016.
- [5] Y. Tabata, "Biomaterial technology for tissue engineering applications," *Journal of the Royal Society Interface*, vol. 6, Supplement_3, pp. S311–S324, 2009.
- [6] S. R. Shin, Y. C. Li, H. L. Jang et al., "Graphene-based materials for tissue engineering," *Advanced Drug Delivery Reviews*, vol. 105, Part B, pp. 255–274, 2016.
- [7] J. Sun and H. Tan, "Alginate-based biomaterials for regenerative medicine applications," *Materials*, vol. 6, no. 4, pp. 1285–1309, 2013.
- [8] W. Yin and D. A. Rubenstein, "Biomedical applications of aerogels," in *Aerogels Handbook*, Advances in Sol-Gel Derived Materials and Technologies, M. Aegerter, N. Leventis, and M. Koebel, Eds., pp. 683–694, Springer, New York, NY, USA, 2011.
- [9] E. Nishida, H. Miyaji, H. Takita et al., "Graphene oxide coating facilitates the bioactivity of scaffold material for tissue engineering," *Japanese Journal of Applied Physics*, vol. 53, no. 6S, article 06JD04, 2014.
- [10] H. I. Chang and Y. Wang, "Cell responses to surface and architecture of tissue engineering scaffolds," in *Regenerative Medicine and Tissue Engineering - Cells and Biomaterials*, pp. 569–588, IntechOpen, 2011.
- [11] J. M. Aamodt and D. W. Grainger, "Extracellular matrix-based biomaterial scaffolds and the host response," *Biomaterials*, vol. 86, pp. 68–82, 2016.
- [12] C. Mao and W. S. Kisaalita, "Characterization of 3-D collagen hydrogels for functional cell-based biosensing," *Biosensors and Bioelectronics*, vol. 19, no. 9, pp. 1075–1088, 2004.
- [13] E. J. Lee, S. H. Jun, H. E. Kim, and Y. H. Koh, "Collagen–silica xerogel nanohybrid membrane for guided bone regeneration," *Journal of Biomedical Materials Research Part A*, vol. 100A, no. 4, pp. 841–847, 2012.
- [14] A. Mandal, S. Sekar, N. Chandrasekaran, A. Mukherjee, and T. P. Sastry, "Synthesis, characterization and evaluation of collagen scaffolds crosslinked with aminosilane functionalized silver nanoparticles: in vitro and in vivo studies," *Journal of Materials Chemistry B*, vol. 3, no. 15, pp. 3032–3043, 2015.
- [15] S. Gorgjeva and V. Kokol, "Collagen- vs. gelatine-based biomaterials and their biocompatibility: review and perspectives," in *Chapter 2, Biomaterials Applications for Nanomedicine*, Intechopen, pp. 17–51, 2011.
- [16] M. L. Foglia, D. E. Camporotondi, G. S. Alvarez et al., "A new method for the preparation of biocompatible silica coated-collagen hydrogels," *Journal of Materials Chemistry B*, vol. 1, no. 45, pp. 6283–6290, 2013.
- [17] M. Kucki, P. Rupper, C. Sarrieu et al., "Interaction of graphene-related materials with human intestinal cells: an in vitro approach," *Nanoscale*, vol. 8, no. 16, pp. 8749–8760, 2016.
- [18] S. Goenka, V. Sant, and S. Sant, "Graphene-based nanomaterials for drug delivery and tissue engineering," *Journal of Controlled Release*, vol. 173, no. 1, pp. 75–88, 2014.
- [19] B. Zhang, Y. Wang, and G. Zhai, "Biomedical applications of the graphene-based materials," *Materials Science and Engineering C*, vol. 61, pp. 953–964, 2016.
- [20] R. Ayranci, G. Başkaya, M. Güzel, S. Bozkurt, F. Şen, and M. Ak, "Carbon based nanomaterials for high performance optoelectrochemical systems," *ChemistrySelect*, vol. 2, no. 4, pp. 1548–1555, 2017.
- [21] S. F. Kiew, L. V. Kiew, H. B. Lee, T. Imae, and L. Y. Chung, "Assessing biocompatibility of graphene oxide-based nanocarriers: a review," *Journal of Controlled Release*, vol. 226, pp. 217–228, 2016.
- [22] R. Deepachitra, V. Ramnath, and T. P. Sastry, "Graphene oxide incorporated collagen–fibrin biofilm as a wound dressing material," *Royal Society of Chemistry Advances*, vol. 4, no. 107, pp. 62717–62727, 2014.
- [23] I. Kanayama, H. Miyaji, H. Takita et al., "Comparative study of bioactivity of collagen scaffolds coated with graphene oxide and reduced graphene oxide," *International Journal of Nanomedicine*, vol. 9, no. 1, pp. 3363–3373, 2014.
- [24] R. J. White, N. Brun, V. L. Budarin, J. H. Clark, and M. M. Titirici, "Always look on the 'light' side of life: sustainable carbon aerogels," *ChemSusChem*, vol. 7, no. 3, pp. 670–689, 2014.
- [25] L. Zuo, Y. Zhang, L. Zhang, Y. E. Miao, W. Fan, and T. Liu, "Polymer/carbon-based hybrid aerogels: preparation, properties and applications," *Materials*, vol. 8, no. 10, pp. 6806–6848, 2015.
- [26] J. A. Burdick and G. Vunjak-Novakovic, "Engineered microenvironments for controlled stem cell differentiation," *Tissue Engineering Part A*, vol. 15, no. 2, pp. 205–219, 2009.
- [27] H. W. Liang, Q. F. Guan, L. F. Chen, Z. Zhu, W. J. Zhang, and S. H. Yu, "Macroscopic-Scale Template Synthesis of Robust Carbonaceous Nanofiber Hydrogels and Aerogels and Their Applications," *Angewandte Chemie International Edition*, vol. 51, no. 21, pp. 5101–5105, 2012.
- [28] Sivaranjani and M. Pandimadevi, "Preparation and characterization of collagen/alginate biocomposite functionalized with graphene oxide for wound healing applications," *International Journal of ChemTech Research*, vol. 10, no. 6, pp. 754–769, 2017.
- [29] D. C. Marcano, D. V. Kosynkin, J. M. Berlin et al., "Correction to synthesis of graphene oxide," *ACS Nano*, vol. 4, no. 8, pp. 4806–4814, 2010.
- [30] M. Quintana, J. I. Tapia, and M. Prato, "Liquid-phase exfoliated graphene: functionalization, characterization, and applications," *Beilstein Journal of Nanotechnology*, vol. 5, no. 1, pp. 2328–2338, 2014.
- [31] S. Some, J. S. Sohn, J. Kim et al., "Graphene-iodine nanocomposites: highly potent bacterial inhibitors that are biocompatible with human cells," *Scientific Reports*, vol. 6, no. 1, article 20015, 2016.
- [32] W. Zhang, H. Sun, Y. Mou et al., "Graphene oxide-collagen matrix accelerated osteogenic differentiation of mesenchymal stem cells," *Journal of Biomaterials and Tissue Engineering*, vol. 5, no. 4, pp. 257–266, 2015.

- [33] L. Baldino, S. Cardea, and E. Reverchon, "Nanostructured chitosan–gelatin hybrid aerogels produced by supercritical gel drying," *Polymer Engineering and Science*, vol. 58, no. 9, pp. 1494–1499, 2018.
- [34] Aerogel.org, "Build a supercritical dryer," February 2019 <http://www.aerogel.org>.
- [35] M. Martins, A. A. Barros, S. Quraishi et al., "Preparation of macroporous alginate-based aerogels for biomedical applications," *Journal of Supercritical Fluids*, vol. 106, pp. 152–159, 2015.
- [36] L. Baldino, S. Concilio, S. Cardea, and E. Reverchon, "Interpenetration of natural polymer aerogels by supercritical drying," *Polymers*, vol. 8, no. 4, p. 106, 2016.
- [37] Z. Bazrafshan and G. Stylios, "High performance of covalently grafting onto collagen in the presence of graphene oxide," *Nanomaterials*, vol. 8, no. 9, p. 703, 2018.
- [38] M. C. Gómez-Guillén, B. Giménez, M. E. López-Caballero, and M. P. Montero, "Functional and bioactive properties of collagen and gelatin from alternative sources: a review," *Food Hydrocolloids*, vol. 25, no. 8, pp. 1813–1827, 2011.
- [39] C. Liu, D. Lewin Mejia, B. Chiang, K. E. Luker, and G. D. Luker, "Hybrid collagen alginate hydrogel as a platform for 3D tumor spheroid invasion," *Acta Biomaterialia*, vol. 75, pp. 213–225, 2018.
- [40] T. Lu, Q. Li, W. Chen, and H. Yu, "Composite aerogels based on dialdehyde nanocellulose and collagen for potential applications as wound dressing and tissue engineering scaffold," *Composites Science and Technology*, vol. 94, pp. 132–138, 2014.
- [41] W. S. Hummers Jr. and R. E. Offeman, "Preparation of graphitic oxide," *Journal of the American Chemical Society*, vol. 80, no. 6, article 1339, 1958.



Hindawi
Submit your manuscripts at
www.hindawi.com

